In situ study of partially crystallized Bioglass® and hydroxylapatite *in vitro* bioactivity using atomic force microscopy

I. B. Leonor,[1] A. Ito,[2] K. Onuma,[2] N. Kanzaki,[2] Z. P. Zhong,[3] D. Greenspan,[3] R. L. Reis[1]
[1]*Department of Polymer Engineering, University of Minho, Campus de Azurém, 4800-058 Guimarães, Portugal*
[2]*Tissue Engineering Research Center, National Institute for Advanced Industrial Science and Technology, Central 4, 1-1-1 Higashi, Tsukuba-shi, Ibaraki 305-8562, Japan*
[3]*US Biomaterials Corporation, One Progress Blvd. £ 23, Alachua, Florida 32615*

Received 2 May 2001; revised 25 January 2002; accepted 13 February 2002

Abstract: The present work investigates, *in situ*, the *in vitro* bioactivity of partially crystallized 45S5 Bioglass® (BG) as a function of immersion time in a simulated body fluid (SBF) using atomic force microscopy (AFM). The results obtained for the crystallized BG® were compared to those of hydroxyapatite c- and a-faces. The calcium phosphate layer grows on the crystallized 45S5 B® by multiple two-dimensional nucleation and fusion of these two-dimensional islands, which is essentially the same mode as for the hydroxyapatite c-face. The surface of the crystallized 45S5 BG® was almost fully covered with a dense and compact calcium phosphate layer after 24 h. The calcium phosphate formation on the crystallized BG® arises from a low surface energy of the surface layer and/or an effect of the layer to lower the resistance when the growth units of calcium phosphate incorporate into the growing island. These results indicate that the crystallized 45S5 BG® is suitable to be used as a filler for polymeric matrix bioactive composites, as it maintains a high bioactivity associated with a stiffer behavior (as compared to standard BG®). © 2002 Wiley Periodicals, Inc. J Biomed Mater Res 62: 82–88, 2002

Key words: Bioglass®; atomic force microscopy; *in situ; in vitro;* bioactivity

INTRODUCTION

The *in vitro* behavior of different types of bioceramics, such as 45S5 Bioglass® (BG®) and hydroxyapatite (HA), has been studied by several investigators.[1–4] These so-called bioactive materials, when immersed in a simulated physiologic solution that mimics the typical ion concentration in body fluids, have the capacity to form a biologically equivalent apatite on their surface.[4–6]

With the invention of atomic force microscope (AFM), one technique in a family of scanning probe microscopes (SPM) by Bining et al. in 1986,[7] it was possible to have a new tool designed to study both conductive and nonconductive surfaces at the atomic level,[8,9] leading to a precise comparison between experiment and theory. The recent improvements in observation and measurement capabilities of this technique include the possibility of scanning the surface under aqueous conditions, which represents a new opportunity to study biomaterials surfaces in chemical environments simulating those found *in vivo*.[9,10]

Nevertheless, to date, only a few efforts have been made to investigate the nucleation and growth kinetics of hydroxyapatite *in situ* by using the AFM. Such type of studies are a very useful tool to understand better the mechanism of the formation of calcium phosphate layers on the surface of a bioactive implant. Examples of such studies have been successfully conducted on a hydroxyapatite single crystal by Onuma et al.[11–14]

The present work investigates the *in vitro* bioactivity of partially crystallized 45S5 BG® as a function of time, by *in situ* observation using AFM. 45S5 BG® was previously sintered at 800°C. The aim of this heat treatment was to obtain a material that is less resorbable, but still bioactive and stiffer than standard BG®. The material is aimed at being used as filler in biodegradable starch based (or other polymers) polymeric matrix composites, as reported previously.[15] Several studies have proved that the incorporation of bonelike

Correspondence to: I. B. Leonor; e-mail: belinha@dep.uminho.pt

inorganic fillers, such as HA or bioactive glasses, on starch based polymers allows for the development of composites that present a degradable behavior, an interesting mechanical behavior that is associated with a clear bioactive character.[16–20] The results obtained for the crystallized BG® were compared to those of hydroxyapatite c- and a-faces.

MATERIALS AND METHODS

Sample preparation

The starting material was a 45S5 Bioglass® (45SBG®) powder with a composition of 45 SiO_2, 24.5 CaO, 24.5 Na_2O, and 6.0 P_2O_5 in wt % (US Biomaterials Corp., FL). Particle size of the 45S5 BG® powder ranged from 38–53 μm as determined by laser scattering analysis using a model Coulter LS 100 particle size analyzer.

Using a steel mould, 0.5 g of 45SBG® powder (not containing any binder) was uniaxially pressed into a disk (10 mm in diameter and 3–4 mm in thickness) at a pressure of 13 MPa for 1 min. The disks were isostatically pressed in a steel mould at a pressure of 15 MPa for 10 min. The green compacts of 45S5 BG® were heated at rates of 20°C min^{-1} up to the sintering temperature of 800°C, then held for 1 h and naturally cooled in the furnace.

The sintered disks were cut into specimens with a size of $1.34 \times 1.03 \times 0.48$ mm^3 for the *in situ* AFM observation using a model ISOMET slow-speed diamond saw (Buehler, USA) and an ISOCUT® fluid. The specimens were cleaned ultrasonically in acetone, rinsed with distilled water, and stored in a desiccator.

In situ AFM experiments

A model Nanoscope III-a Scanning Probe Microscope System (Digital Instruments Inc., Santa Barbara, CA) was used to observe the surface of the 45S5 BG® and HA specimens in a fluid cell filled with a simulated body fluid (SBF), at pH 7.35, that had ion concentrations similar to those of human plasma (Table I) The *in situ* observation was performed in the contact mode at 25°C for 48 h using silicon-nitride (Si_3N_4) cantilevers with a spring constant of 0.58 N/m and an E-type (a 10 μm scanning range) piezo scanner. The SBF was renewed every 24 h. After the *in situ* observation, the specimens were carefully cleaned with distilled water and dried at 23°C under a constant relative humidity of 55%.

In vitro bioactivity tests

Standard *in vitro* bioactivity tests[22,23] were performed in combination with the *in situ* AFM observation. The sintered 45S5 BG® disks (with a size 10 mm in diameter and 3–4 mm in thickness) were soaked in 15 mL of SBF in 15 mL polypropylene sterile tubes for 0, 15 min, 1, 4, 8, and 10 h, and 1, 2, 3, and 7 days at 37°C and pH 7.35. After soaking, the specimens were immediately cleaned with distilled water and dried at 23°C under a constant relative humidity of 55%.

Surface analysis

The surface morphology was analyzed by scanning electron microscopy (SEM) before and after the immersion in the SBF in order to complement the *in situ* AFM observation. Prior to any SEM observations, all the specimens were sputter coated with gold by ion sputtering (Sputter JEOL JFC 1100 equipment). The phases present in the 45S5 BG® were identified by thin-film X-ray diffraction (TF-XRD) before and after the sintering. Surface roughness of the specimens was measured as a function of immersion time in the SBF using the software installed in the AFM. The area of growth island was measured by an image analysis system. The diameter of the growth island was calculated from the measured area. Chemical composition of the surface was measured by X-ray photoelectron spectroscopy (XPS; Model ESCALAB2201-XL X-ray photoelectron spectrometer; Thermo VG Scientific, East Grinstead, England) using monochromated-AlKα at 10 kV and 16 mA and HA and tricalcium phosphate ceramic disks as references of chemical composition. The measured area was approximately 600 μm in diameter and 3 nm in depth.

Solution analysis

Evolution of Ca, P, Si, and Na ion concentrations and pH of the SBF were determined as a function of immersion time. The ion concentrations were measured by inductively coupled plasma emission (ICP) spectroscopy.

RESULTS

The 45S5 BG® was completely amorphous in structure before the sintering at 800°C (Fig. 1). However, the 45S5 BG® almost fully crystallized into $Na_2Ca_2Si_3O_9$

TABLE I
Ion Concentration of SBF and Human Blood Plasma[21]

	Na^+	K^+	Ca^{2+}	Mg^{2+}	Cl^-	HCO_3^-	HPO_4^{2-}	SO_4^{2-}
SBF	142.0	5.0	2.5	1.5	147.8	4.2	1.0	0.5
Human plasma	142.0	5.0	2.5	1.5	103.0	27.0	1.0	0.5

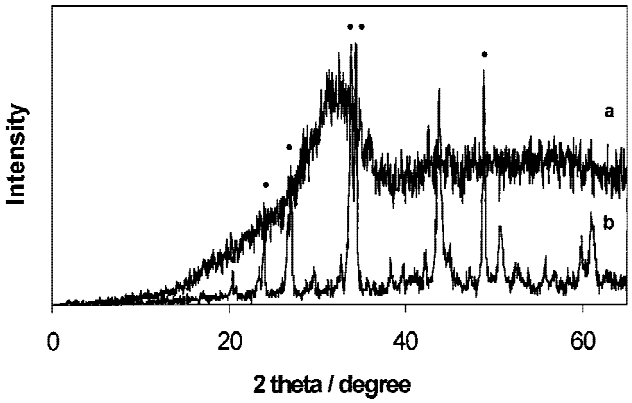

Figure 1. XRD patterns of the Bioglass® nonsintered (a) and after sintering (b). ($Na_2Ca_2Si_3O_9$).

after the sintering as previously reported by other authors.[24,25]

The *in situ* AFM observation (Fig. 2) revealed that a calcium phosphate layer grows on the crystallized 45S5 BG® through the following three stages:

Stage 1: rapid formation of island structure on the surface ($0 < T < 15$ min).

Stage 2: increase in number of the islands (15 min $< T < 4$ h).

Stage 3: fusion of the islands (4 h $< T$).

In Stage 1, an island structure was formed on the 45S5 BG® within the initial 15 min with a density of 16.3 islands per square micron. The average diameter of randomly selected 16 islands was 0.28 ± 0.06 μm. No significant increase in diameter (0.30 ± 0.05 μm) was observed for these islands after 1 h. During the initial 15 min, surface roughness decreased significantly by 48% (Fig. 3). Presence of Ca, P, Mg, and Na on the surface was demonstrated by XPS. Si was detected by XPS in some areas of the surface but not in another areas. Ca/P molar ratios of 2.6 and 2.2 were observed in the areas where Si was detected and not detected, respectively. The presence of Mg indicated reaction between the SBF and the crystallized 45S5 BG® because the SBF is the only source of Mg. In Stage 2, the number of islands increased up to 4 h (Fig. 4).

The increase in the number of islands as a function of immersion time up to 4 h was regressed as

$$N = 115T^{0.233} \quad (0 < T < 4) \tag{1}$$

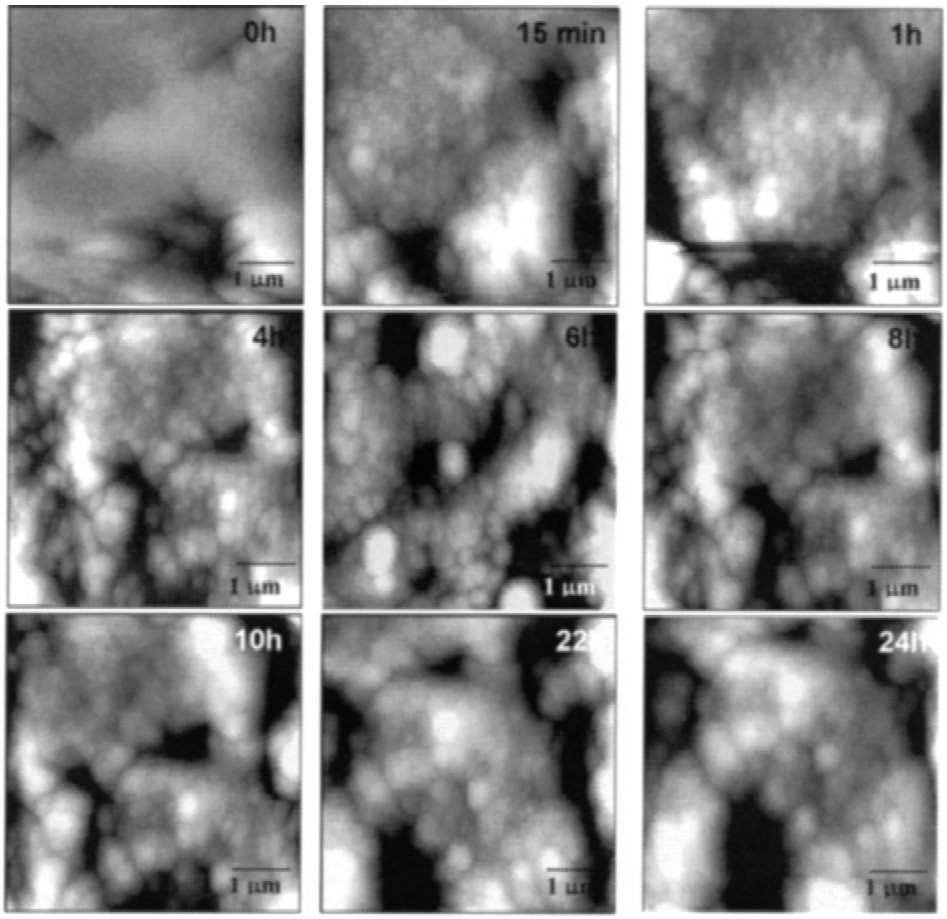

Figure 2. AFM images showing the formation of Ca-P layer on the surface of 45S5 Bioglass® *in situ*.

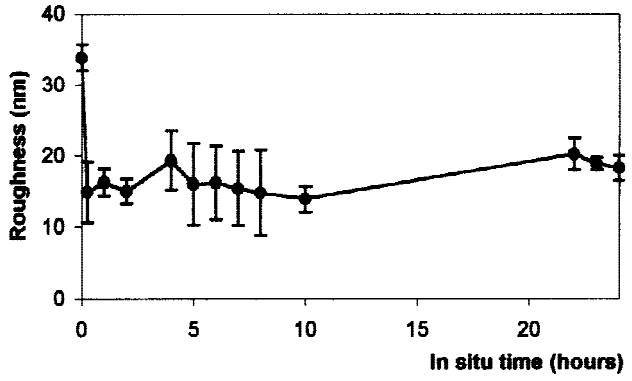

Figure 3. Changes of the roughness of 45S5 Bioglass® surface as a function of *in situ* immersion time.

where N and T are the number of the islands and the immersion time in hour, respectively. After 4 h, fusion of islands became predominant rather than an increase in the number of islands (Table II).

The process of island fusion was a stochastic process, which was best regressed by the following equation:

$$N = 453T^{-0.786} \quad (4 < T < 24) \tag{2}$$

During the initial 15 min, there was no obvious change in silicon concentration of the SBF (Fig. 5). In the period between 15 min and 4 h, calcium and sodium concentrations increased slightly, indicating the occurrence of ion exchange between calcium and sodium in the glass network and the intake of H^+ from the solution. After 4 h immersion, calcium and phosphorus concentrations decreased rapidly with increases in sodium and silicon concentrations in the SBF. After 24 h, the pH of the SBF increased to 8.20 from the initial value of 7.35.

The surface of the crystallized 45S5 BG® was almost fully covered with a calcium phosphate layer after 24 h as revealed by SEM observation [Fig. 6(b)].

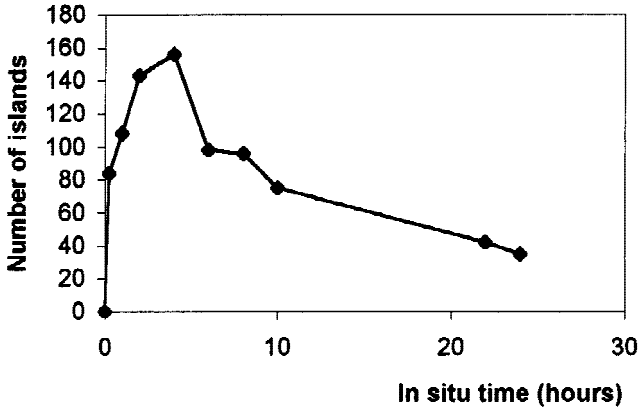

Figure 4. Changes in the number of islands on the 45S5 Bioglass® surface as a function of *in situ* immersion time.

DISCUSSION

The formation and growth of the calcium phosphate on the crystallized 45S5 BG® differs from those on hydroxyapatite. On hydroxyapatite c-face, a two-dimensional island with a size of approximately 10 nm and with a Ca/P molar ratio of 1.50 appears within 5 min in an SBF (Table III).[12] The c-face of hydroxyapatite grows by multiple two-dimensional nucleation growth in which many calcium phosphate islands nucleate independently before one island spreads and completely covers the crystal face. In the case of the crystallized 45S5 BG®, islands with a size of 278 nm appeared within 15 minutes. There is no direct evidence showing that the islands are either those of grown calcium phosphate, or those formed by rapid and uneven surface dissolution. Nevertheless, calcium phosphate is likely to be formed and partly cover the surface during this stage because a Ca/P molar ratio of 2.2 was observed by XPS in some areas where Si was not detected.

Between 15 min and 4 h, the number of islands increased gradually. These islands nucleated independently before one island spread and covered the surface completely, which is essentially the multiple two-dimensional nucleation growth. The islands formed on the crystallized 45S5 BG® between 15 min and 4 h in the present study are probably amorphous calcium phosphate deposited on the SiO_2-rich layer.[1,2,26,27]

Although the number of islands increases on the crystallized BG® up to 4 h immersion, on hydroxyapatite it starts to decrease only after some minutes by the fusion of the islands.

The calcium phosphate formation on the crystallized BG® arises from a low surface energy of the surface layer and/or an effect of the layer to lower the resistance when the growth unit of calcium phosphate incorporates into the growing island. As proposed by Hench et al.,[2,4,26,28,29] the first reaction of this type of bioactive glass surface is ion exchange, in which Ca^{2+} and Na^+ in the glass exchange for H^+ in the solutions, resulting in an increase in pH of the solution as well as formation of a hydrated silica gel layer. It is also reported that the hydrated silica layer on the surface of Bioglass® provides favorable sites for the calcium phosphate nucleation.[2,27,30] The rate of nucleation, J, obtained by differentiating the Equation (1)

$$J = dN/dT = 27.0T^{-0.766} \tag{3}$$

is an exponential function of time, which decreases monotonously as time increases. This Equation (3) is unchanged even if a constant, which corresponds to the number of islands formed not by growth but by rapid and uneven surface dissolution before 15 min, is

TABLE II
Typical Example of Change in Area of Islands (μm^2) As a Function of Immersion Time

	Immersion Time (h)					
Islands	2	4	5	8	10	22
N2	0.1375	0.1444	0.1361	0.1305		
N5	0.1031	0.1002	0.1098	0.1143	0.2776	
N6	0.0770	0.0713	0.0714	0.0720	0.0681	0.0742
N7	0.0734	0.0594	0.0645	0.0575	0.0630	
N8	0.2009	0.1685	0.2080	0.2187	0.2157	0.3751
N12	0.0947	0.0905				
N13	0.0492	0.0711	0.2878	0.2427	0.3193	0.3391
N16	0.1027	0.0982				
N17	0.0374	0.0310	0.1532	0.1234		
N18	0.0633	0.0467	0.0680			
N19	0.0445	0.0544	0.0522	0.1569	0.35074	0.38220

Arrows represent the fusion of islands.

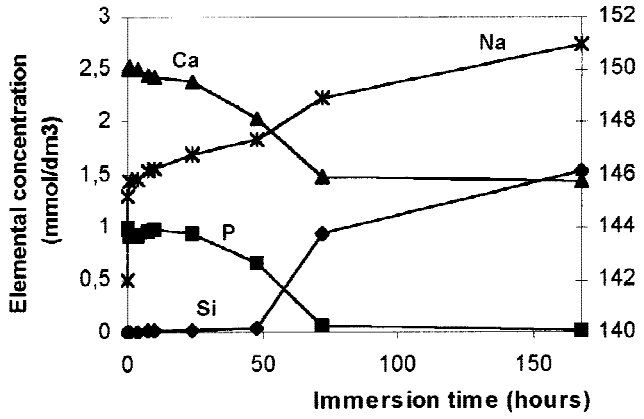

Figure 5. Evolution of Ca, P, Si, and Na elemental concentrations (ICP results) in the SBF solution as a function of the immersion time for 45S5 Bioglass® samples.

subtracted from N. On the other hand, the J at a fixed time is known to be expressed as

$$J = AC(\Delta\mu/kT)^{1/2}\, exp(-\Delta U/kT)exp(-\pi\gamma^2/kT\Delta\mu) \quad (4)$$

for the multiple two-dimensional nucleation growth, where A, C, $\Delta\mu$,k, T, ΔU and γ are a constant, concentration of apatite in the SBF, chemical potential, Boltzmann constant, temperature, energy of desolvation, and edge free energy, respectively.[31] Using the following relations:

$$C = Ce(\sigma + 1)$$

$$\Delta\mu/kT = \ln(\sigma + 1)$$

$$\exp(-\Delta U/kT) = D\beta$$

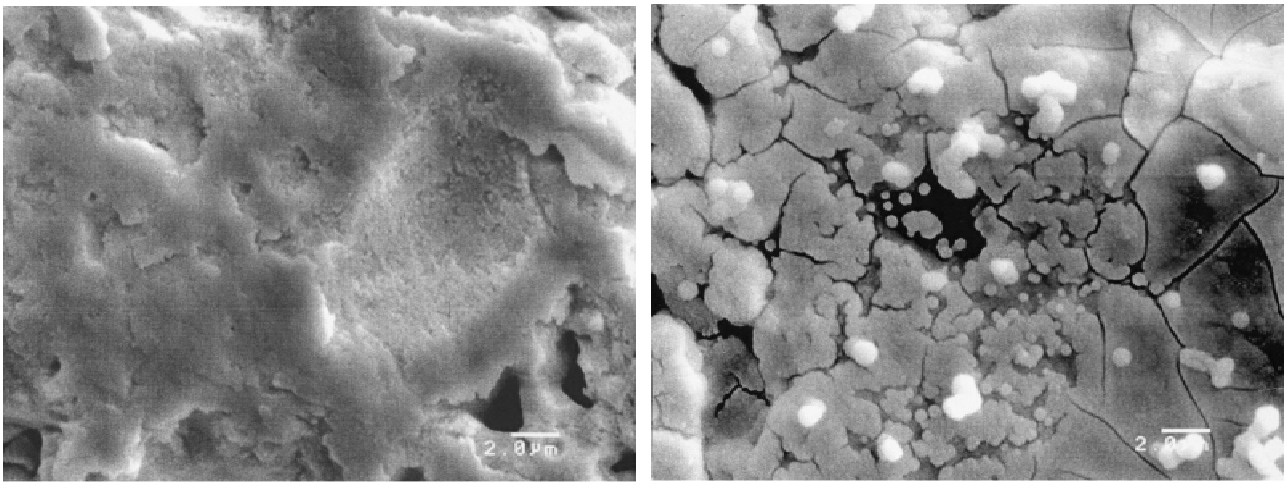

Figure 6. SEM micrographs showing the formation of a Ca-P layer on the surface of 45S5 BG® after (a) 0 and (b) 24 h of immersion in SBF.

TABLE III
Comparison of Island Diameter, Lateral Growth Rate, and Nucleation Density

Substrate	Island Diameter (mm)	Lateral Growth Rate (pm/s)	Nucleation Density (μm^{-2})	Solution	pH	Immersion Time (min)	Ref.
Crystallized BG	278 ± 5	—	16.25	SBF	7.35	15	
HAP c-face	9.1 ± 1.4	30 ± 4	5570 ± 823	Mg-CO_3-SBF[a]	7.40	5	11
HAP c-face	10.1 ± 1.2	17 ± 2	4136 ± 954	Mg-CO_3-SBF	7.40	10	12
HAP c-face	17.5 ± 3.1	—	3604 ± 634	Mg-CO_3-SBF	7.40	120	11
HAP c-face	14.2 ± 3.0	—	2781 ± 471	CO_3-SBF[b]	7.40	240	13
HAP a-face	—	52–76	—	Mg-CO_3-SBF	7.40	120	14

[a]Mg-CO_3-SBF: Magnesium and carbonate-free SBF.
[b]CO_3-SBF: carbonate-free SBF.

where Ce, σ, D, and β are equilibrium solubility of apatite, supersaturation, a constant, and kinetic coefficient, respectively, Equation (4) leads to

$$J = A'Ce\,(\sigma + 1)\beta\,\{ln\,(\sigma + 1)\}^{1/2}\,exp[-\pi\gamma^2/\{(kT)^2\ln(\sigma + 1)\}] \quad (5)$$

where A' is a constant. Equation (5) means that the rate of nucleation, J, is controlled by three factors, σ, β, and γ, because Ce is a constant. The increase in pH and Ca concentration caused by the reaction of crystallized BG® results in an increase in σ, and hence results in an increase in J. Therefore, the increase in σ with increasing time does not account for the monotonous decrease in J shown by Equation (3). The monotonous decrease in J observed in the present study should result from a change in β and/or γ. The kinetic coefficient, β, is the reciprocal of relative resistance of direct incorporation of growth unit into growing island, and the edge free energy, γ, is proportional to surface energy. Therefore, the monotonous decrease in nucleation rate, J, should mean an increase in resistance of direct incorporation and/or an increase in surface energy with an increase in time. This means that the formation of calcium phosphate on the SiO_2-rich layer should arise from a low surface energy of the layer and/or an effect of the layer to lower the resistance when the growth unit of calcium phosphate incorporates into the growing island. These effects of SiO_2-rich layer would weaken as the calcium phosphate layer covers the surface. It has been reported[2,4,28,29,32] that the early precipitation of Ca and P in SBF obstructed the further ion exchange and the further formation of silica gel layer on Bioglass®, thus slowing down the surface reaction stages, including the change in pH and surface area, as well as hydroxycarbonate apatite formation.

After 4 h of immersion, a rapid drop of Ca and P concentration in the solution was observed resulting in an increase in Na and Si concentration in the solution. This stage corresponds to the crystallization stage of hydroxycarbonate apatite. The two-dimensional islands fuse spontaneously by consuming the calcium and phosphate ions in the solution that is supersaturated with respect to apatite. In this stage, surface morphology changes especially between 4 and 6 h. In the present study, it took 24 h to obtain a calcium phosphate layer on the surface of the crystallized BG®. SBF bioactivity tests for 45S5 glass-ceramic with different contents of crystalline phase, varying from 8–100%, showed that a partially crystalline carbonated apatite layer was formed on the surface after 20–24 h regardless of the content of crystalline phase,[4,24,33] although the rate of hydroxycarbonate apatite formation was increased for the glass-ceramics with lower crystallinities.

CONCLUSIONS

The surface of the partially crystallized 45S5 BG® was almost fully covered with a calcium phosphate layer after 24 h. The calcium phosphate layer grows on the partially crystallized 45S5 BG® by multiple two-dimensional nucleation and fusion of these islands after an incubation period. The calcium phosphate formation on the partially crystallized BG® arises from a low surface energy of the surface layer and/or an effect of the layer to lower the resistance when the growth unit of calcium phosphate incorporates into the growing island.

References

1. Hench LL. Bioceramics: From concept to clinic. J Am Ceram Soc 1991;74:1487–1510.
2. Hench LL, Anderson Ö. Bioactive glasses. In: Hench LL, Wilson J, editors. An introduction to bioceramics. Singapore: World Scientific; 1993. p 41–62.
3. LeGeros RZ, LeGeros JP. Dense hydroxyapatite. In: Hench LL, Wilson J, editors. An introduction to bioceramics. Singapore: World Scientific; 1993. p 139–180.
4. Hench LL. Bioactive ceramics. In: Ducheyne P, Lemons JE, editors. Bioceramics: Material characteristics versus in vivo behaviour. New York: New York Academy of Sciences; 1988. p 54–71.
5. Ducheyne P, Qiu Q. Bioactive ceramics: the effect of the surface

reactivity on bone formation and bone cell function. Biomaterials 1999;20:2287–2303.
6. Cao W, Hench LL. Bioactive materials. Ceramics Int 1986;22: 493–507.
7. Bining G, Quante CF, Gerber CH. Atomic force microscope. Phys Rev Lett 1986;56:930–933.
8. Leung OM, Goh MC. Orientational ordering of polymers by atomic force microscope tip-surface interaction. Science 1992; 255:64–66.
9. Ratner BD. Characterization of biomaterial surfaces. Cardiovasc Pathol 1993;2:87S–100S.
10. Siedlecki CA, Marchant RE. Atomic force microscopy for characterization of the biomaterials interface. Biomaterials 1998;19: 441–454.
11. Onuma K, Kanzaki N, Ito A, Tateishi T. Growth kinetics of the hydroxyapatite (0001) face revealed by phase shift interferometry and atomic force microscopy. J Phys Chem B 1998;102: 7833–7838.
12. Kanzaki N, Onuma K, Ito A, Teraoka K, Tateishi T, Tsutsumi S. Direct growth rate measurement of hydroxyapatite single crystal by moire phase shift interferometry. J Phys Chem B 1998; 102:6471–6476.
13. Kanzaki N, Onuma K, Treboux G, Tsutsumi S, Ito A. Inhibitory effect of magnesium and zinc on crystallization kinetics of hydroxyapatite (0001) face. J Phys Chem B 2000;104:4189–4194.
14. Onuma K, Ito A, Tateishi T, Kameyama T. Growth kinetics of hydroxyapatite crystal revealed by atomic force microscopy. J Crystal Growth 1995;154:118–125.
15. Leonor IB, Sousa RA, Cunha AM, Zhong ZP, Greenspan D, Reis RL. Development of highly bioactive and mechanically strong starch thermoplastic/Bioglass® composite biomaterials. In: Giannini S, Moroni A, editors. Bioceramics, Volume 13. Zurich: Trans Tech Publications; 2000. p 705–708.
16. Sousa RA, Reis RL, Cunha AM, Bevis MJ. Structure and properties of hydroxylapatite reinforced starch bone-analogue composites. In: Giannini S, Moroni A, editors. Bioceramics, Volume 13. Zurich: Trans Tech Publications; 2000. p 669–672.
17. Reis RL, Cunha AM, Allan PS, Bevis MJ. Structure development and control of injection-molded hydroxylapatite-reinforced starch/EVOH composites. J Polym Adv Techn 1997; 16:263–277.
18. Reis RL, Cunha AM, Bevis MJ. Using nonconventional processing to develop anisotropic and biodegradable composites of starch-based thermoplastics reinforced with bone-like ceramics. Med Plast Biomater 1997;4:46–50.
19. Reis RL, Leonor IB, Rego MT, Cunha AM, Fernandes MH, Correia RN. Stiff and bioactive composites based on starch, polyethylene and SiO_2-CaO.P_2O_5-MgO glasses and glass-ceramics. In: LeGeros RZ, LeGeros JP, editors. Bioceramics, Volume 11. New York: World Scientific; 1998. p 169–172.
20. Mano JF, Vaz CM, Mendes SC, Reis RL, Cunha AM. Dynamic mechanical properties of hydroxyapatite-reinforced and porous starch-based degradable biomaterials. J Mater Sci Mater Med 1999;10:857–862.
21. Tanahashi M, Hata K, Kokubo T, Minoda M, Miyamoto T, Nakamura T. Effect of substrate on apatite formation by a biomimetic process. In: Yamamuro T, Kokubo T, Nakamura T, editors. Bioceramics, Volume 5. Kyoto: Kobunshi-Kankokai, Inc.; 1992. p 57–64.
22. Kokubo T, Kushitani H, Sakka S, Kitsugi T, Yamamuro T. Solutions able to reproduce in vivo surface-structure changes in bioactive glass-ceramic A-W. J Biomed Mater Res 1990;24:721–734.
23. Ducheyne P, Qiu Q. Bioactive ceramics: the effect of surface reactivity on bone formation and bone cell function. Biomaterials 1999;20:2287–2303.
24. Filho OP, LaTorre GP, Hench LL. Effect of crystallization on apatite-layer formation of bioactive glass 45S5. J Biomed Mater Res 1996;30:509–514.
25. Rizkalla AS, Jones DW, Clarke DB, Hall GC. Crystallization of experimental bioactive glass compositions. J Biomed Mater Res 1996;32:119–124.
26. Filgueiras MR, LaTorre G, Hench LL. Solution effects on the surface reactions of a bioactive glass. J Biomed Mater Res 1993; 27:445–453.
27. Wen HB, Moradian-oldak J, Zhong JP, Greenspan DC, Fincham AG. Effects of amelogenin on the transforming surface microstructures of Bioglass® in a calcifying solution. J Biomed Mater Res 2000;52:762–773.
28. Hench LL, LaTorre GP. Reaction kinetics of bioactive ceramics Part IV: Effect of glass and solution composition. In: Yamamuro T, Kokubo T, Nakamura T, editors. Bioceramics, Volume 5. Kyoto: Kobunshi-Kankokai, Inc.; 1992. p 67–74.
29. Hench LL. Bioactive glasses and glass-ceramics: A Perspective. In: Yamamuro T, Hench LL, Wilson J, editors. Handbook of Bioactive Ceramics, Volume I. Boston: CRC Press; 1990. p 7–23.
30. Li P, Ohtsuki C, Kokubo T, Nakanishi K, Soga N, Nakamura T, Yamamuro T. Effects of ions in aqueous media on hydroxyapatite induction by silica gel and its relevance to bioactivity of bioactive glasses and glass-ceramics. J Appl Biomater 1993;4: 221–229.
31. Markov IV. Crystal growth for beginners. Singapore: World Scientific; 1995. p 107.
32. Zhong JP, Greenspan DC. Bioglass® surface reactivity: From in vitro to in vivo. In: LeGeros RZ, LeGeros JP, editors. Bioceramics, Volume 11. New York: World Scientific; 1998. p 415–418.
33. Rehman I, Karsh M, Hench LL, Bonfield W. Analysis of apatite layers on glass-ceramic particulate using FTIR and FT-Raman spectroscopy. J Biomed Mater Res 2000;50:97–100.